Self-calibrating measurement of polarization-dependent frequency shifts from Rb-^{3}He collisions

A. S. Barton, N. R. Newbury,* G. D. Cates, B. Driehuys, H. Middleton, and B. Saam
Department of Physics, Princeton University, Princeton, New Jersey 08544
(Received 27 May 1993)

We have studied the frequency shift in the Rb electron-paramagnetic-resonance (EPR) line due to the presence of nuclear polarized ^{3}He. By measuring the resonant frequency in a cylindrical cell oriented both parallel and perpendicular to an applied magnetic field, we determined the classical EPR shift due to long-range macroscopic fields. We thus calibrated the larger, geometry-independent shift, due to the Fermi-contact interaction between the Rb electron and the ^{3}He nucleus, to 2.5%. The EPR frequency shift can be used to determine the ^{3}He nuclear polarization.

PACS number(s): 32.80.Bx, 32.30.Dx, 33.25.−j, 33.35.−q

I. INTRODUCTION

The technique of producing high polarizations in ^{3}He through spin exchange with optically pumped Rb vapor has become widely used in atomic [1,2], nuclear [3–5], and high-energy [6] physics experiments. Many of these experiments require absolute measurements of the ^{3}He polarization. Shifts of the electron-paramagnetic-resonance (EPR) line in Rb due to interactions with nuclear polarized ^{3}He can be used for polarimetry [1, 7]. Calibration of these shifts has traditionally relied on measurements of the noble-gas magnetization [7, 8]. In this paper we present an alternative method for calibrating the shift of the Rb EPR line in the presence of nuclear polarized ^{3}He. This technique, in which we measure both a classical geometric shift and the shift due to the Fermi-contact interaction between the Rb valence electron and the ^{3}He nucleus, has the advantage that the ^{3}He magnetization drops out in the final analysis. Thus we are insensitive to the density and absolute polarization of our sample. Our technique therefore results in the most precise measurement to date of κ_0, the parameter that characterizes the Fermi-contact shift.

Both the geometric and Fermi-contact shifts are proportional to the nuclear polarization of the ^{3}He. In general, the magnitude of the classical geometric shift in the Rb depends on the orientation of the magnetization with respect to the geometry. By measuring the EPR frequency for two orientations of a cylindrical geometry, with respect to an applied magnetic field, we separate the classical geometric shift from the shift due to the Fermi-contact interaction. We note that for spherical geometry there is no long-range shift. The classical shift acts as a calibration which allows us to determine the relationship between the ^{3}He polarization and the shift due to the Fermi-contact interaction without a direct measurement of the ^{3}He polarization or density.

In the presence of polarized high-pressure ^{3}He gas, Rb EPR lines are shifted by several mechanisms. In our samples, the dominant (~10 kHz) shifts are caused by the Fermi-contact interaction between the Rb valence electron and the ^{3}He nucleus, and the geometry-dependent long-range dipole-dipole interaction [9]. Light shifts [10], Rb-Rb spin-exchange shifts [11,12], the Bloch-Siegert shift [13], and shifts due to magnetic-field inhomogeneities [14] are typically only a few Hz and are thus negligible in comparison. (We note that this is during the measurement cycle where our resonant light power is ~10 μW and the Rb number density is $\sim 10^{12}$ atoms cm^{-3}.)

II. THEORY

A detailed description of the quantum mechanical origins of frequency shifts in alkali-metal atoms due to the presence of nuclear polarized noble gases can be found in the literature [8, 15, 16]. Here we will concentrate on the use of these shifts and the classical long-range shifts to determine κ_0, the parameter that characterizes the shift due to the Fermi-contact interaction. The Fermi-contact interaction $\alpha\mathbf{K}\cdot\mathbf{S}$ between the electron spin $\mathbf{S}$ of an alkali-metal atom and the nuclear spin $\mathbf{K}$ of a polarized noble-gas atom causes a frequency shift in the EPR line of the alkali-metal atom. The same interaction causes a frequency shift in the NMR line of the noble-gas atom in the presence of a polarized alkali-metal vapor. These shifts, respectively, can be characterized by the dimensionless enhancement factors κ_{AX} and κ_{XA} [7, 17].

In general, both van der Waals molecules and binary collisions contribute to κ_{AX} and κ_{XA}. At high enough pressures where binary collisions dominate the enhancement factors approach a common limiting value $\kappa_{AX} = \kappa_{XA} \equiv \kappa_0$, as defined by Schaefer *et al.* [7]. This limit is valid for all of our helium samples. For Rb-He interactions, the shift $\Delta\nu_{FC}$ in the Rb EPR line due to the Fermi-contact interaction can be expressed as [8]

*Present address: JILA, Boulder, CO 80309.

$$\Delta\nu_{\rm FC} = \frac{\mu_B g_s}{h(2I+1)}\kappa_0\frac{8\pi}{3}\mu_{\rm He}[{\rm He}]\frac{\langle K_z\rangle}{\mathbf{K}}, \quad (1)$$

where μ_B is the Bohr magneton, [He] is the ^{3}He number density, I is the nuclear spin of the relevant Rb isotope, $g_s \approx 2$ is the electron g factor, and $\mu_{\rm He}$ is the ^{3}He nuclear magnetic moment.

If we rewrite the helium nuclear polarization in terms of the magnetization M, the shift in the Rb EPR frequency due to the Fermi-contact interaction becomes

$$\Delta\nu_{\rm FC} = \kappa_0\left(\frac{\gamma_{\rm Rb}}{2\pi}\right)\frac{8\pi}{3}M, \quad (2)$$

where $\gamma_{\rm Rb}$ is the Rb gyromagnetic ratio.

An additional geometric shift for nonspherical geometries arises from the long-range magnetic field created inside the cell due to the polarized gas [19]. As illustrated in Fig. 1, for an infinite cylinder of uniform magnetization M aligned to an applied magnetic field along the cylinder axis, the long-range magnetic field $B_\parallel$ adds to the applied field. For M and the applied magnetic field perpendicular to the cylinder axis, the long-range field $B_\perp$ subtracts from the applied field. The long-range field $B_\parallel$ ($B_\perp$) at any point $\mathbf{x}_0$ in the cell is

$$B_\parallel(B_\perp) = \int_0 \frac{3\hat{n}(\vec{M}\cdot\hat{n}) - \vec{M}}{|\mathbf{x}-\mathbf{x}_0|^3}dV - \frac{8\pi}{3}\vec{M}, \quad (3)$$

where the short-range contribution to the integral at $\mathbf{x}=\mathbf{x}_0$, which we have treated quantum mechanically, (2), has been subtracted. The integral can be evaluated most simply by converting (3) to a surface charge integral. For an infinite cylinder we find, $B_\parallel = 4\pi M$ and $B_\perp = -2\pi M$. The total shift in the Rb EPR line will be the sum of the classical depolarization shift [9] due to (3), and the shift due to the contact interaction given by (2) such that

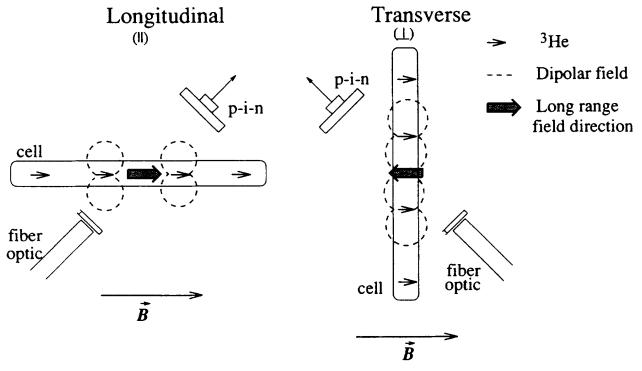

FIG. 1. Sample cell shown in both the longitudinal and transverse positions. The small arrows indicate ^{3}He spins aligned along the applied magnetic field $\vec{B}$. In the center of each cell a large arrow indicates the direction of the long-range contribution to the magnetic field. For the longitudinal case, the long-range field due to the ^{3}He spins adds to the applied magnetic field, while in the transverse case the long-range field subtracts from the applied field.

$$\Delta\nu_\parallel = \frac{\gamma_{\rm Rb}}{2\pi}\left(\frac{8\pi}{3}\kappa_0 M + 4\pi M\right), \quad (4)$$

$$\Delta\nu_\perp = \frac{\gamma_{\rm Rb}}{2\pi}\left(\frac{8\pi}{3}\kappa_0 M - 2\pi M\right). \quad (5)$$

Note that in a sphere $B_\parallel$ and $B_\perp$ are zero and $\Delta\nu_\parallel$ and $\Delta\nu_\perp$ are both given by Eq. (2).

From (2) and (3) it follows that

$$\kappa_0 = \frac{3}{4}\left(\frac{\Delta\nu_\parallel}{\widetilde{\Delta\nu}}\right) - \frac{1}{2}, \quad (6)$$

where $\widetilde{\Delta\nu} = \Delta\nu_\parallel - \Delta\nu_\perp$. We can therefore measure κ_0 without any *a priori* knowledge of the magnetization M.

III. EXPERIMENTAL APPARATUS

The experiment was performed on a 7 inch long cylindrical cell with a 3/4 inch diameter. The cell, made of Corning aluminosilicate glass, contained about 8 amagats of ^{3}He, a few milligrams of Rb metal, and about 75 Torr of nitrogen. The ^{3}He was polarized by spin exchange with optically pumped Rb vapor [15, 16, 21, 22] while the cell was heated to 175–200 °C in a pumping oven to maintain a Rb number density of $\sim 4\times10^{14}\,{\rm cm}^{-3}$. Two Spectra Physics Ti:Sapphire lasers provided 4 W each of resonant Rb D_1 light at 795 nm. A series of cylindrical lenses expanded the beam to conform to the size and shape of that cell. The buildup of the ^{3}He polarization was monitored by a fast passage NMR setup [23]. Once the ^{3}He was polarized to ~20%, it was transferred to a measurement oven controlled at 74.5±5.0 °C ([Rb]$\sim 10^{12}$ cm^{-3}) inside a set of Helmholtz coils. The magnetic field was locked to 1 G using a Cs magnetometer [8].

Since the cell was large with considerable surface area, we needed to modify the filling techniques described in Refs. [1, 24] to ensure a long ^{3}He nuclear spin relaxation time. Specifically, we cleaned the raw tubing with nitric acid before constructing the cell and baked the completed cell under vacuum at 450 °C for 24 h before filling. The 16.4 h cell lifetime was not limited by ^{3}He-^{3}He collisions [24], but was sufficient for this work.

Figure 2(a) shows the apparatus used to measure the Rb EPR frequency. A detailed discussion of the mechanism used to measure the EPR frequency is given in Ref. [8]. Circularly polarized light from a Rb discharge lamp was directed to the cell through a fiber optic. The circularly polarized light polarized the Rb vapor. The transmission of this light through the cell, which is dependent on the Rb polarization, was measured by applying a rf magnetic field oscillating at the Rb EPR frequency. Typical linewidths were on the order of 5 kHz. The applied radio frequency was locked to the Rb EPR frequency as shown in Fig. 2(b). Since the [Rb] during this measurement was low ($\sim 10^{12}\,{\rm cm}^{-3}$), any Rb polarization had negligible effect on the ^{3}He polarization or the shift in the Rb EPR line.

The measurement oven pivoted about the center of the cell so that the helium spins, which remain fixed along the magnetic field, could be oriented both parallel and

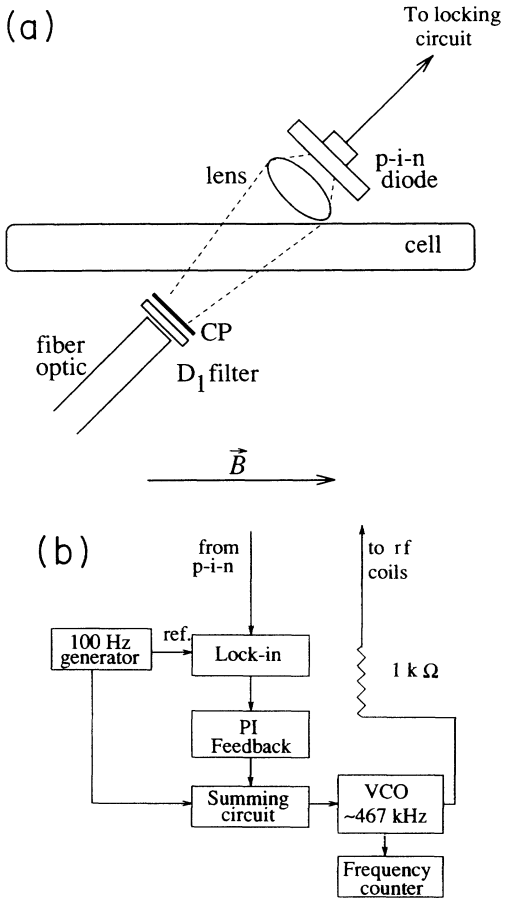

FIG. 2. (a) Apparatus used in locking to the Rb EPR frequency. The fiber optic in combination with the circular polarizer (CP), and the D_1 filter delivered resonant 795 nm light. Transmission of the light was monitored by a *p-i-n* diode whose signal was used in the locking circuit shown in (b). The rf coils, not shown in this figure, were mutually perpendicular to the magnetic-field axis and the light axis. (b) Circuit used to lock to the Rb EPR frequency. PI indicates a proportional and integrating feedback circuit and VCO indicates a voltage controlled oscillator.

perpendicular to the cylinder axis (Fig. 1). The magnetic field at the sampling region was fixed along the cell axis in the longitudinal position by adjusting the current through orthogonal Helmholtz coils while measuring the field with a three-axis Bartington flux-gate magnetometer.

As indicated in Fig. 1, the light traveled at an angle of 45° to the cylinder axis. Although reducing the signal by a factor of $\sqrt{2}$, this angle allowed us to fix the position of the frequency locking apparatus with respect to the cell. The fiber optic, the lens, the *p-i-n* diode, and the rf coils were mounted to move with the cell as it rotated. Therefore the sampled region was identical in both the longitudinal and transverse positions. The only systematic errors due to rotating the cell resulted from magnetic-field gradients near the pivot point, which were measured to be less than 1 mG/cm.

IV. ANALYSIS

The Rb EPR frequency was measured for a polarized ^{3}He cylinder in the longitudinal and transverse positions. The resonance frequency was measured in a series of five runs consisting of 2–14 sets of frequency measurements. Each set consisted of a 1–2 min measurement in each of the two positions. The frequency measurement apparatus remained locked during each complete run. After each polarized run, a similar run was taken with an unpolarized cell of virtually the same dimension to determine a baseline Rb EPR frequency. We had previously determined that this cell and the polarized cell gave the same baseline frequency. During these baseline runs, the polarized cell was removed from the measurement oven to a holding field which preserved the polarization. Polarization loss during this transfer did not affect the analysis because each run was analyzed separately.

The frequency shift, $\Delta\nu_\parallel$ or $\Delta\nu_\perp$, was obtained for each position in each run by subtracting the unpolarized baseline frequency from the frequency measured with the polarized cell. The frequency measurements in the two positions were then subtracted to determine $\widetilde{\Delta\nu}$. We also corrected for polarization decay. The decay time constant, 16.40 ± 0.16 h, was measured by locking to the Rb EPR frequency while the cell was in the longitudinal position over a period of over 12 h.

The parameter κ_0 can only be determined from these measurements if we correct Eq. (6) for the finite size of the cylinder. Corrections to the values of $B_\parallel$ and $B_\perp$ of $\approx 2.0\%$ at the sampling region were determined by using the scalar potential method for hard magnets [20]. The longitudinal case was solved analytically using a first order expansion in the ratio of the cylinder radius to the cylinder length. The ratio for our cylinder was about 1/20, and a first order expansion was accurate to about

TABLE I. The quantities $\Delta\nu_\parallel$, $\Delta\nu_\perp$, $\widetilde{\Delta\nu}_{\text{expt}}$, and κ_0 determined from each data run. The analysis of this data includes a 2.0% correction for the finite size of the cylinder. The errors given are purely statistical. With systematic errors included, the average shifts yield a value of $\kappa_0 = 5.13 \pm 0.13$ at 74.5 °C. The shifts are negative because the spins were aligned antiparalleled to the applied magnetic field.

Run	$\Delta\nu_\parallel$ (Hz)	$\Delta\nu_\perp$ (Hz)	$\widetilde{\Delta\nu}_{\text{expt}}$ (Hz)	κ_0
1	-9565 ± 12	-8261 ± 24	-1283 ± 5	5.00 ± 0.04
2	-7892 ± 11	-6856 ± 21	-1009 ± 10	5.27 ± 0.03
3	-6885 ± 36	-5989 ± 21	-916 ± 24	5.06 ± 0.08
4	-3279 ± 8	-2859 ± 10	-422 ± 6	5.25 ± 0.08
5	-2829 ± 13	-2456 ± 11	-370 ± 7	5.15 ± 0.11

one part in 10^4. The transverse case was solved numerically to the same accuracy.

Our largest error was incurred from uncertainties in the baseline frequencies measured in the longitudinal and transverse positions. Two methods of baseline subtraction were used to calculate $\Delta\nu_{\|}$ and $\Delta\nu_{\perp}$. With the first method, the unpolarized baseline measurements for each position were averaged over all of the runs to determine a global baseline for the longitudinal position of 455 030±100 Hz and the transverse position of 455 090±100 Hz. (Magnetic-field gradients could cause the small difference in baseline frequencies because in each position a slightly different spatial region is sampled.) With the second method, only the baseline measurements preceding and following each run were used. Both baseline subtraction methods yield the same value for κ_0. The 100 Hz error bars encompass all long term drifts in the baseline due to changing magnetic fields.

The next largest systematic error in the measurement of κ_0 comes from a temperature gradient of 1.3 °C/cm along the length of the cylinder. Based on measurements of the temperature dependence of κ_0 by Newbury *et al.* [8], an average temperature in the sampling region with a conservative uncertainty (74.5±5.0 °C) introduces a 1% error to the measurement.

Other systematics did not contribute significantly to the error in κ_0. First, the ^{3}He cell was not completely cylindrical. Fabrication techniques [24] required that there was a "pulloff" of volume 0.50±0.05 cm^3 located near one end of the cylinder. We estimated the effect of the polarized helium in this pulloff by modeling it as a dipole. The shift in the Rb EPR frequency in either cell orientation due to this volume was less than 1%. Second, if the magnetic fields perpendicular to the 1 G quantization axis are not adequately canceled, the direction of the magnetization with respect to the cylinder axis is changed. This results in a modification of $B_{\|}$ and $B_{\perp}$ which will introduce an error in κ_0. The perpendicular magnetic-field components were measured to be less than 20 mG and contributed negligibly to the overall error.

Table I indicates the values of $\Delta\nu_{\|}$, $\Delta\nu_{\perp}$, $\widetilde{\Delta\nu}_{\rm expt}$, and κ_0 for each run. The quantity $\widetilde{\Delta\nu}_{\rm expt}$ is defined as the difference of two sequential measurements. Since the measurements alternated between two positions, a given longitudinal measurement was associated with both the preceding and following transverse measurement. The quantity $\widetilde{\Delta\nu}_{\rm expt}$ was calculated by averaging both differences. By defining $\widetilde{\Delta\nu}_{\rm expt}$ in this way, we became less sensitive to drifts in the baseline frequency which are clearly visible in Fig. 3. Figure 3 is a graph of $\Delta\nu_{\|}$ and $\Delta\nu_{\perp}$ for the first data run. The data are corrected only for polarization decay and are calculated using the global baseline.

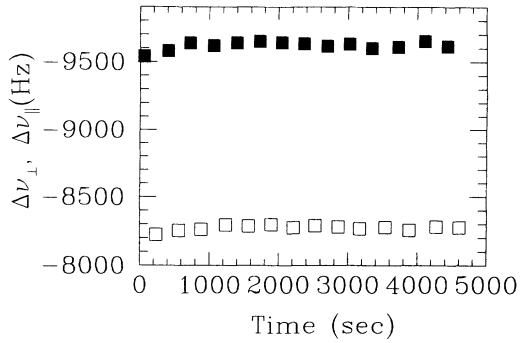

FIG. 3. The quantities $\Delta\nu_{\|}$ (filled) and $\Delta\nu_{\perp}$ (hollow) corrected for polarization decay as defined in Eqs. (4) and (5) for a single run. Each point represents 1–2 min of frequency-locked data for either the longitudinal or transverse position. The error bars, which are smaller than the point size, are purely statistical and do not include the systematic 100 Hz baseline error.

V. CONCLUSION

We have calibrated the shift in the Rb EPR line due to the Fermi-contact interaction with a gas of polarized ^{3}He. The parameter κ_0 which characterizes this shift is measured to be

$$\kappa_0 = 5.13 \pm 0.13 \tag{7}$$

at 74.5 °C.

Given the 2.5% accuracy in κ_0, the measurement of the Rb EPR shift in the presence of polarized ^{3}He can be used as a precise form of polarimetry. An important feature of this experiment is the fact that we combined measurements of the classical geometric shift and the quantum mechanical Fermi-contact shift to determine κ_0, thus eliminating sensitivity to the density of the sample. Our result is not only more accurate than previous measurements, it is fundamentally different than those calibrations which relied on NMR techniques because it requires no direct measurement of the magnetization M. (For a discussion of the relative merits of these two techniques, see Ref. [8].) This technique can be applied to measurements of κ_0 for other alkali-metal–noble-gas systems.

[1] N. R. Newbury *et al.*, Phys. Rev. Lett. **67**, 3219 (1991); **69**, 391 (1992).
[2] T. E. Chupp and R. J. Hoare, Phys. Rev. Lett. **64**, 2261 (1990); T. E. Chupp *et al.*, *ibid.* **63**, 1541 (1989).
[3] A. K. Thompson *et al.*, Phys. Rev. Lett. **68**, 2901 (1992).
[4] B. Larson *et al.*, Phys. Rev. Lett. **67**, 3356 (1991).
[5] K. P. Coulter *et al.*, Nucl. Instrum. Methods Phys. Res. **A 288**, 463 (1990).
[6] P. L. Anthony *et al.*, Phys. Rev. Lett. **71**, 959 (1993).
[7] S. R. Schaefer, G. D. Cates, Ting-Ray Chien, D. Gonatas,

W. Happer, and T. G. Walker, Phys. Rev. A **39**, 5613 (1989).
[8] N. R. Newbury, A. S. Barton, P. Bogorad, G. D. Cates, M. Gatzke, H. Mabuchi, and B. Saam, Phys. Rev. A **48**, 558 (1993).
[9] J. A. Osborn, Phys. Rev. **67**, 153 (1945); R. M. Bozarth and D. M. Chapin, J. Appl. Phys. **12**, 320 (1942).
[10] W. Happer and S. Svanberg, Phys. Rev. A **9**, 508 (1974).
[11] W. Happer and H. Tang, Phys. Rev. Lett. **31**, 273 (1973).
[12] L. C. Balling, R. J. Hanson, and F. M. Pipkin, Phys. Rev. **133**, A607 (1964); L. C. Balling and F. M. Pipkin, *ibid.* **136**, A46 (1964).
[13] F. Bloch and A. Siegert, Phys. Rev. **57**, 522 (1940).
[14] G. D. Cates, S. R. Schaefer, and W. Happer, Phys. Rev. A **37**, 2877 (1988).
[15] W. Happer, Rev. Mod. Phys. **44**, 169 (1972).
[16] W. Happer, E. Miron, S. Schaefer, D. Schreiber, W. A. van Wijngaarden, and X. Zeng, Phys. Rev. A **29**, 3092 (1984).
[17] B. C. Grover, Phys. Rev. Lett. **40**, 391 (1978).
[18] J. D. Jackson, *Classical Electrodynamics* (John Wiley and Sons, Inc., New York, 1975), p. 184.
[19] C. Kittel and H. Kroemer, *Thermal Physics* (W. H. Freeman and Company, New York, 1980).
[20] For a discussion of the scalar magnetic potential, and the contribution of the δ-function piece of the dipolar magnetic field, see p. 194 of Ref. [18].
[21] X. Zeng, Z. Wu, T. Call, E. Miron, D. Schreiber, and W. Happer, Phys. Rev. A **31**, 260 (1985).
[22] T. E. Chupp, M. E. Wagshul, K. P. Coulter, A. B. McDonald, and W. Happer, Phys. Rev. C **36**, 2244 (1987).
[23] C. P. Slichter, *Principles of Magnetic Resonance* (Harper and Row, New York, 1963), pp. 26–44.
[24] N. R. Newbury, A. S. Barton, G. D. Cates, W. Happer, and H. Middleton, Phys. Rev. A **48**, 4411 (1993).

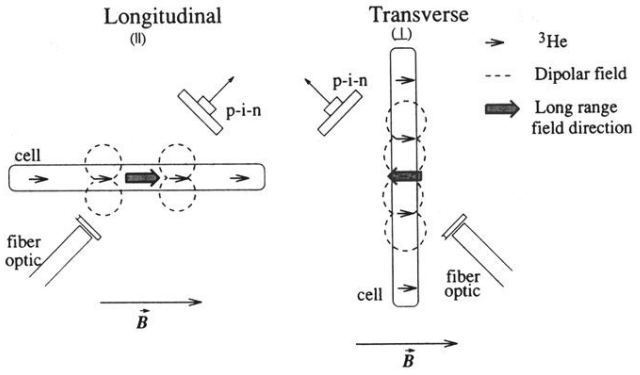

FIG. 1. Sample cell shown in both the longitudinal and transverse positions. The small arrows indicate ^{3}He spins aligned along the applied magnetic field $\vec{B}$. In the center of each cell a large arrow indicates the direction of the long-range contribution to the magnetic field. For the longitudinal case, the long-range field due to the ^{3}He spins adds to the applied magnetic field, while in the transverse case the long-range field subtracts from the applied field.